The Journal of Neuroscience, June 15, 1997, 17(12):4711–4721

An ATP-Dependent Inwardly Rectifying Potassium Channel, K_{AB}-2 (Kir4.1), in Cochlear Stria Vascularis of Inner Ear: Its Specific Subcellular Localization and Correlation with the Formation of Endocochlear Potential

Hiroshi Hibino,[1,2] Yoshiyuki Horio,[1] Atsushi Inanobe,[4] Katsumi Doi,[2] Minoru Ito,[4] Mitsuhiko Yamada,[1] Takahiro Gotow,[3] Yasuo Uchiyama,[3] Masaru Kawamura,[5] Takeshi Kubo,[2] and Yoshihisa Kurachi[1,4]

Departments of [1]Pharmacology II, [2]Otolaryngology, and [3]Anatomy I, Faculty of Medicine, Osaka University, Osaka 565, Japan, [4]Department of Cell Biology and Signaling, Yamagata University School of Medicine, Yamagata 990-23, Japan, and [5]Department of Biology, University of Occupational and Environmental Health, Kitakyushu 807, Japan

Cochlear endolymph has a highly positive potential of approximately +80 mV. This so-called endocochlear potential (EP) is essential for hearing. Although pivotal roles of K^+ channels in the formation of EP have been suggested, the types and distribution of K^+ channels in cochlea have not been characterized. Because EP was depressed by vascular perfusion of Ba^{2+}, an inhibitor of inwardly rectifying K^+ (Kir) channels, but not by either 4-aminopyridine or tetraethylammonium, we examined the expression of Kir channel subunits in cochlear stria vascularis, the tissue that is supposed to play the central role in the generation of positive EP. Of 11 members of the Kir channel family examined with reverse transcription-PCR, we could detect only expression of K_{AB}-2 (Kir4.1) mRNA in stria vascularis. K_{AB}-2 immunoreactivity was specifically localized at the basolateral membrane of marginal cells but not in either basal or intermediate cells. Developmental expression of K_{AB}-2 in marginal cells paralleled formation of EP. Furthermore, deaf mutant mice (*viable dominant spotting*; W^V/W^V) expressed no K_{AB}-2 in their marginal cells. These results suggest that K_{AB}-2 in marginal cells may be critically involved in the generation of positive EP.

Key words: inwardly rectifying potassium channel; endocochlear potential; stria vascularis; vestibule; development; W^V/W^V mice

The cochlear endolymph of inner ear has a highly positive potential of approximately +80 mV, which is called endocochlear potential (EP). In addition, the endolymph is an unusual extracellular fluid containing 150 mM K^+, 2 mM Na^+, and 20 μM Ca^{2+} (Morgenstern et al., 1982). Cochlear hair cells expose their stereocilia to endolymph and bathe their bodies in an ordinary extracellular fluid, perilymph. Upon mechanical stimulation, K^+ ions flow into hair cells through mechanosensor channels at the tips of cilia, excite cells, and release the neurotransmitter glutamate (for review, see Ashmore, 1991). The positive EP facilitates K^+ influx by increasing its driving force, resulting in high sensitivity of hair cells to mechanical stimulation (Dallos, 1978). The positive EP, therefore, seems to be essential for auditory function.

Generation of high concentrations of K^+ ($[K^+]$) and positive EP in endolymph has been considered to occur at cochlear stria vascularis (Tasaki and Spyropoulos, 1959). Stria vascularis contains three types of cells: marginal, basal and intermediate. Marginal cells form a continuous layer facing the endolymph, whereas the layer of basal cells borders the spiral ligament filled with perilymph. Intermediate cells and capillaries are scattered between the two layers. Various ion transporters and channels that may be responsible for the generation of EP and endolymphatic high $[K^+]$ exist in these cells.

Na^+,K^+-ATPase and $Na^+,K^+,2Cl^-$ cotransporter that are localized at the basolateral membrane of marginal cells contribute to the generation of EP, because ouabain and furosemide, specific blockers of Na^+,K^+-ATPase and $Na^+,K^+,2Cl^-$ cotransporter, respectively, depressed EP (Kusakari et al., 1978; Konishi and Mendelsohn, 1970). In vestibule, on the other hand, endovestibular fluid also contains 150 mM K^+, but its potential is ~0 mV, although dark cells, corresponding to cochlear marginal cells, also express both Na^+,K^+-ATPase and $Na^+,K^+,2Cl^-$ cotransporter at their basolateral membrane (Schulte and Adams, 1989; Marcus et al., 1994). Therefore, the pump and cotransporter are obligatory but insufficient for generation of EP. Because vascular perfusion of Ba^{2+} dramatically reduces EP and because no basal cells exist in vestibule, a K^+ conductance localized on basal cells in stria vascularis has been supposed to be essential for EP formation (Marcus et al., 1985; Salt et al., 1987); however, the types and distribution of the K^+ channels involved in generation of EP in stria vascularis have not been identified.

We propose that an inwardly rectifying K^+ (Kir) channel, K_{AB}-2 (Kir4.1), is critically involved in Ba^{2+} inhibition of EP. K_{AB}-2 was the only Kir channel subunit that could be detected to be expressed in stria vascularis among 11 members of the Kir

Received Jan. 21, 1997; revised March 17, 1997; accepted March 31, 1997.

This work was partly supported by grants from the Ministry of Education, Culture, Sports and Science of Japan, and the "Research for the Future" Program in the Japan Society for the Promotion of Science (JSPS-RFTF96L00302). We thank Professor Shin-ichi Nishikawa and Dr. Hisahiro Yoshida (Kyoto University Faculty of Medicine) for their kind guidance in whole-mount immunohistochemistry technique, Dr. Ian Findlay (Université de Tours, France) for the critical reading of this manuscript, and Ms. Chiaki Matsubara for technical assistance. We also thank Dr. Sergio Gloor (Swiss Federal Institute of Technology, Switzerland) for kind provision of anti-β2 subunit of Na^+,K^+-ATPase, and Professor Wolfgang Schwarz (Max-Planck-Institut für Biophysik, Germany) for help with immunohistochemistry.

Correspondence should be addressed to Y. Kurachi, Department of Pharmacology II, Faculty of Medicine, Osaka University, 2–2 Yamadaoka, Suita, Osaka 565, Japan.

Table 1. The nucleotide positions of primers and protocols of PCR reactions

Names of channels	Positions of primers	Base pairs of bands	Protocols of PCR
ROMK1 (Kir1.1)	67 ~ 84, 522 ~ 538	472	94°C, 45 sec; 60°C, 1 min 30 sec; 72°C, 2 min
	*793 ~ 812, 1100 ~ 1119	327	94°C, 1 min; 68°C, 1 min; 72°C, 2 min
IRK1 (Kir2.1)	1232 ~ 1249, 1517 ~ 1534	303	94°C, 1 min; 58°C, 1 min 15 sec; 72°C, 2 min
IRK2 (Kir2.2)	1288 ~ 1305, 1523 ~ 1539	252	94°C, 1 min; 68°C, 1 min; 72°C, 1 min 30 sec
	*152 ~ 172, 847 ~ 866	715	94°C, 1 min; 68°C, 1 min; 72°C, 2 min
IRK3 (Kir2.3)	304 ~ 323, 1198 ~ 1223	820	94°C, 1 min; 68°C, 1 min; 72°C, 1 min
GIRK1 (Kir3.1)	1192 ~ 1209, 1492 ~ 1509	318	94°C, 1 min; 57°C, 1 min 30 sec; 72°C, 2 min
GIRK2 (Kir3.2)	914 ~ 933, 1259 ~ 1277	364	94°C, 1 min; 64°C, 1 min; 72°C, 2 min
GIRK3 (Kir3.3)	611 ~ 630, 1048 ~ 1067	457	94°C, 1 min; 64°C, 1 min; 72°C, 2 min
GIRK4 (Kir3.4)	904 ~ 923, 1246 ~ 1265	362	94°C, 1 min; 68°C, 1 min; 72°C, 1 min
	*4 ~ 22, 362 ~ 380	377	94°C, 1 min; 63°C, 1 min 30 sec; 72°C, 1 min 40 sec
K_{AB}-2/BIR10 (Kir4.1)	312 ~ 329, 966 ~ 983	672	94°C, 45 sec; 60°C, 1 min; 72°C, 2 min
uK_{ATP}-1 (Kir6.1)	566 ~ 583, 943 ~ 959	394	94°C, 1 min; 68°C, 1 min; 72°C, 1 min 30 sec
	*401 ~ 418, 704 ~ 722	322	94°C, 1 min; 63°C, 1 min 30 sec; 72°C, 1 min 40 sec
BIR (Kir6.2)	198 ~ 215, 623 ~ 642	445	94°C, 1 min; 60°C, 1 min; 72°C, 1 min

The sets of primers indicated by asterisks were also used, but the data were not shown in Figure 2.

channel family examined in this study. It was specifically localized in cochlear marginal cells at their basolateral membrane but not in vestibular dark cells. Developmentally, expression of K_{AB}-2 in stria vascularis started after endolymphatic high $[K^+]$ had been established and increased to a plateau with a similar time course as the development of EP. Deaf mutant mice (*viable dominant spotting*, W^V/W^V), whose EP is ~0 mV, expressed no K_{AB}-2 in their stria vascularis. This is the first report of the identity of the ion channel that may be involved in the generation of EP.

MATERIALS AND METHODS

Measurement of EP. Healthy albino guinea pigs (200–250 gm) (SLC, Hamamatsu, Japan) were anesthetized intramuscularly with pentobarbital sodium (Nembutal; Abbott, Chicago, IL), paralyzed by intravenous injection of pancuronium bromide (3 mg/kg), and artificially respired. The right cochlea was exposed with a ventrolateral approach. EP on the right side was measured with a glass microelectrode filled with 160 mM KCl solution, inserted into the scala media of the second turn through the spiral ligament (see Fig. 1, *inset*). Vascular perfusion of the stria vascularis was performed at a rate of 1.5 ml/min through a polyethylene tube located in the right vertebral artery.

Control perfusate contained (in mM): 136.5 NaCl, 5.4 KCl, 1.8 $CaCl_2$, 0.53 $MgCl_2$, 5.5 glucose, and 5.0 HEPES-NaOH buffer, pH 7.4. Barium chloride and 4-aminopyridine (4-AP) were dissolved in control solution before use. When 40 mM tetraethylammonium (TEA) chloride was used, the NaCl concentration was adjusted to maintain the correct osmotic pressure. Two syringe pumps were used to inject solutions: one was for control solution and the other was for the solution containing blockers. After injection of a blocker, control solution (~4 ml) was immediately perfused at a rate of 1.5 ml/min.

Reverse transcription (RT)-PCR analyses and in situ *hybridization histochemistry of K_{AB}-2 in rat cochlea.* Total RNA from whole cochleae of female adult Sprague Dawley (SD) rats (130–170 gm) (SLC) was extracted by guanidine thiocyanate methods (Glisin et al., 1974). cDNA was synthesized using oligo-(dT) primers after treatment of RNA with deoxyribonuclease (DNase) I. Each PCR reaction was performed in a volume of 30 μl. For each reaction, 0.8 μg total RNA of whole cochlea was used. Stria vascularis was isolated as follows. Female adult SD rats (130–170 gm) were anesthetized. The ear capsules were exposed and broken out, and then cochlear lateral walls with stria vascularis and spiral ligament were isolated. Stria vascularis from all turns of cochleae were separated from spiral ligament with a fine needle in cold PBS. The pieces of isolated stria vascularis from 42 ears were suspended in 30 μl of 10 mM Tris-HCl, 1 mM EDTA, pH 7.4. They were frozen rapidly with dry ice and thawed twice. Then DNase I and tRNA (10 μg) were added to the mixture in the presence of ribonuclease inhibitor and incubated for 15 min at 37°C. After incubation, the mixture was treated with proteinase K for 30 min at 55°C and then for 10 min at 70°C. RNA was treated with phenol and chloroform, and precipitated with ethanol. The RNA thus obtained was used to synthesize cDNA, 1/20 of which was used for one PCR reaction (30 μl). The nucleotide positions of primers specific to cDNA of different inwardly rectifying K^+ (Kir) channel subunits and the protocols of each PCR reaction are depicted in Table 1. All PCR reactions were performed for 30 cycles. In the analysis of stria vascularis mRNA, two rounds of amplification by PCR were performed. In the second round, 4 μl of the first PCR products was used and amplified with the same primers and the same condition as in the first reaction. For positive control reactions, cDNA of each Kir channel subunit was used as a template. All PCR products were analyzed by a 2% agarose gel. Ethidium bromide was used for staining of PCR products. To increase the sensitivity for detection of PCR products, SYBR Green I (FMC Bio Products, Rockland, ME), which is at least 25 times more sensitive than ethidium bromide, was also used. Nucleotide sequences of the PCR products from whole cochlea were performed using a sequencer (A-381; Applied Biochemicals, Foster City, CA) with dye termination method.

In situ hybridization of cochlear cryosections (10 μm thick) was performed essentially as described previously (Takumi et al., 1995). After fixation with 4% paraformaldehyde/0.1 M sodium phosphate, pH 7.4, isolated cochleae were decalcified in EDTA solution (9% EDTA 2 Na, 10% EDTA 4 Na, pH 7.4) at 4°C for 5 d.

Immunohistochemistry. Adult female SD rats (SLC) were used in whole-mount and slice immunohistochemistry and in immunogold electronmicroscopic examination. In developmental studies, SD rats at different ages were examined. In double-immunostaining, W^V/W^V mice (SLC) and adult ddY mice (SLC) were used.

Affinity-purified anti-K_{AB}-2C2 antibody, which was raised against the amino acid sequence in the C-terminal end of rat K_{AB}-2 (EKEGSALSVRISNV), was prepared as reported previously (Ito et al., 1996). Anti-K_{AB}-2C2 antibody can recognize both rat and mouse K_{AB}-2, because the amino acid sequence in the C-terminal end of mouse K_{AB}-2 is identical with that of rat K_{AB}-2 (our unpublished observations). Anti-mouse β2 subunit of Na^+,K^+-ATPase (adhesion molecule on glia) monoclonal antibody was kindly provided by Dr. Sergio Gloor (Department of Neurobiology, Swiss Federal Institute of Technology, Zürich, Switzerland).

Whole-mount immunohistochemistry was performed according to Yoshida et al. (1996) with anti-K_{AB}-2C2 antibody (0.1 μg/ml) and ABC kit (Vectastain Elite ABC kit; Vector Laboratories, Burlingame, CA). Stained cochleae were examined using a stereoscope (WILD M10; Leica, Heerbrugg, Switzerland).

Slice immunohistochemistry was performed as described previously (Ito et al., 1996). The cryosections were incubated with anti-K_{AB}-2C2 antibody (0.08 μg/ml) and treated with ABC kit (Vector Laboratories) or fluorescein isothiocyanate (FITC)-labeled anti-rabbit antibody. Nuclei were stained with hematoxylin after immunostaining. Negative control sections were treated with anti-K_{AB}-2C2 antibody with an excess of the antigen oligopeptide. In double-immunostaining, we confirmed that

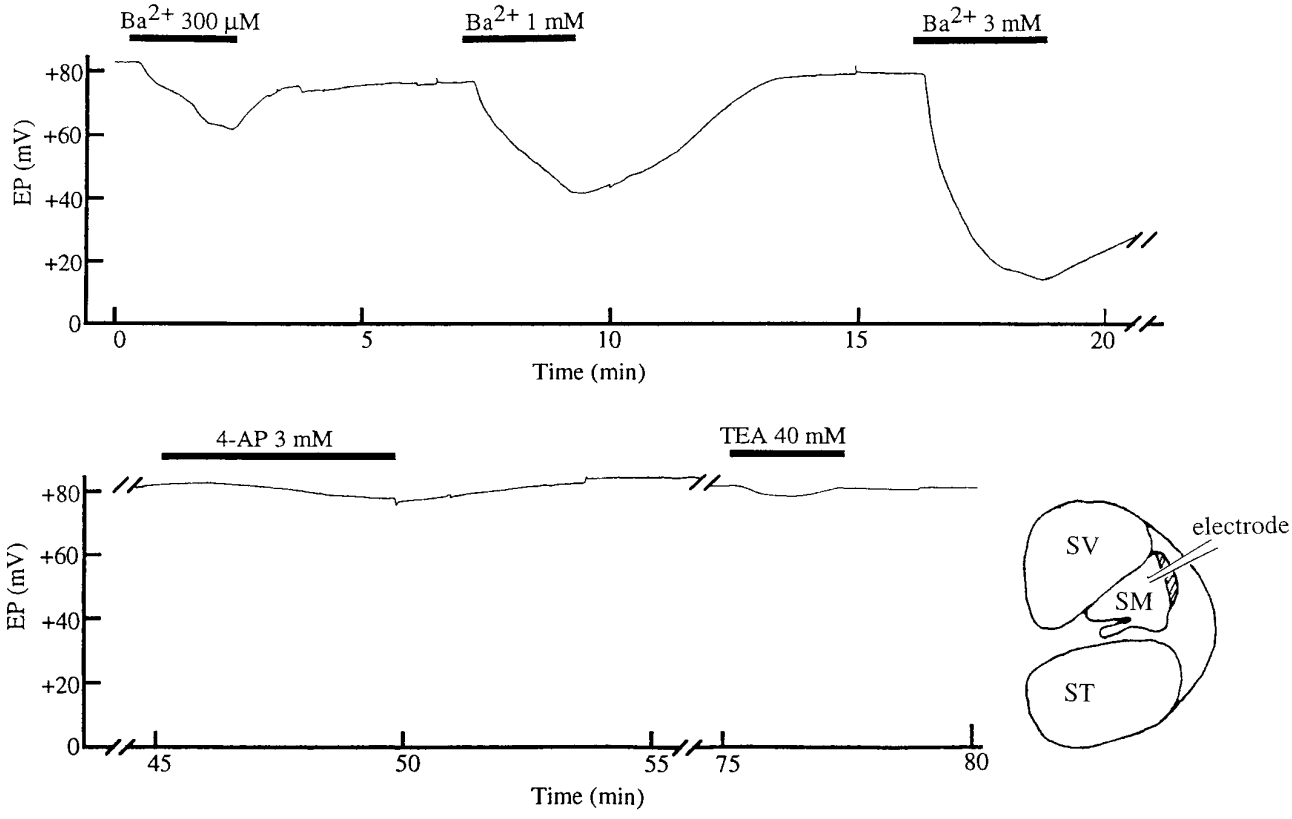

Figure 1. Effects of blockers of various K^+ channels on endocochlear potential (*EP*). The EP of guinea pig was measured with a glass microelectrode inserted into scala media (*inset*). The blockers were perfused into a vertebral artery for the periods indicated by the *bars*. *4-AP*, 4-aminopyridine; *TEA*, tetraethylammonium; *SV*, scala vestibuli; *SM*, scala media; *ST*, scala tympani.

W^V/W^V mice were almost deaf by measurement of their auditory evoked brainstem response before fixation. Cochlear sections were treated with both anti-K_{AB}-2C2 and anti-β2 subunit of Na^+,K^+-ATPase antibodies and incubated with FITC and Texas Red-labeled secondary antibodies. Confocal images were obtained under a laser scanning microscope (MRC-1024; Bio-Rad, Hertfordshire, England).

The method of preembedding immunogold (5 nm) electronmicroscopy was almost the same as that reported previously (Gotow et al., 1995). Small fixed blocks of stria vascularis were immersed in 2.3 M sucrose in 0.1 M phosphate buffer and frozen in liquid nitrogen. Cryothin sections were cut on a microtome equipped with cryoattachment (OmU4, Reichert, Vienna, Austria) and collected on formvar carbon-coated grids. These cryothin sections on grids were incubated with anti-K_{AB}-2C2 antibody (8 μg/ml) and with goat anti-rabbit IgG coupled to 5 nm colloidal gold particles (Amersham, Buckinghamshire, England). The sections were again fixed with 2% glutaraldehyde and post-fixed with 1% O_SO_4, stained with 0.5% uranyl acetate, dehydrated in ethanol, and embedded in London Resin white.

RESULTS

Effects of blockers of K^+ channels on EP

To estimate which types of K^+ channels might be crucially involved in the generation of the highly positive EP, we perfused three kinds of K^+ channel blockers, Ba^{2+}, a nonselective blocker of inwardly rectifying K^+ (Kir) channels, and 4-AP and TEA, blockers of voltage-dependent K^+ (K_V) channels, into a right vertebral artery while measuring EP in guinea pig (Fig. 1). Capillaries in the stria vascularis diverge from the anterior inferior cerebellar artery, one of the branches of the vertebral artery. Thus, the blockers were probably applied to intermediate cells, the basolateral surface of marginal cells, and the apical side of basal cells in the stria vascularis.

EP under control conditions was +84 mV in the example shown in Figure 1. Perfusion of Ba^{2+} (300 μM–3 mM) caused rapid (<1 min) and prominent decline of EP in a dose-dependent fashion, as reported previously (Marcus et al., 1985). Continuous perfusion of Ba^{2+} for 2 min depressed EP by 20.5 ± 2.1 mV at 300 μM, 41.3 ± 4.1 mV at 1 mM, and 71 ± 2.6 mV at 3 mM (mean ± SD; n = 4). These responses were reversible (Fig. 1). On the other hand, perfusion of high concentrations of 4-AP (3 mM) or TEA (40 mM) had little effect on EP (n = 4) (Fig. 1, *bottom panel*). The Ba^{2+}-induced depression of EP is likely, therefore, to be the result of inhibition of Kir channels and not K_V channels, although high concentrations of Ba^{2+} could also inhibit K_V channels.

RT-PCR analyses and *in situ* hybridization histochemistry

The Kir channel family has more than 10 members (Doupnik et al., 1995). To identify which Kir channel subunits are expressed in cochlea, the RT-PCR analysis of rat cochlear total RNA was performed using specific sets of primers for 11 Kir channel subunits: K_{AB}-2 (Kir4.1), ROMK1 (Kir1.1), GIRK1–4 (Kir3.1–3.4), IRK1–3 (Kir2.1–2.3), uK_{ATP}-1 (Kir6.1), and BIR (Kir6.2) (Fig. 2*A*). These primers can identify all Kir channel subunits reported so far, with the exception of BIR9 (Kir5.1). Because BIR9 alone did not form a functional Kir channel (Bond et al., 1994), in this study we have examined all of the subunits that cover practically all functional Kir channels cloned so far.

Each set of primers amplified its specific DNA fragment when cDNA of each Kir channel subunit was used as a template (Fig. 2*A*, Table 1). We found that five Kir channel subunits, i.e., K_{AB}-2

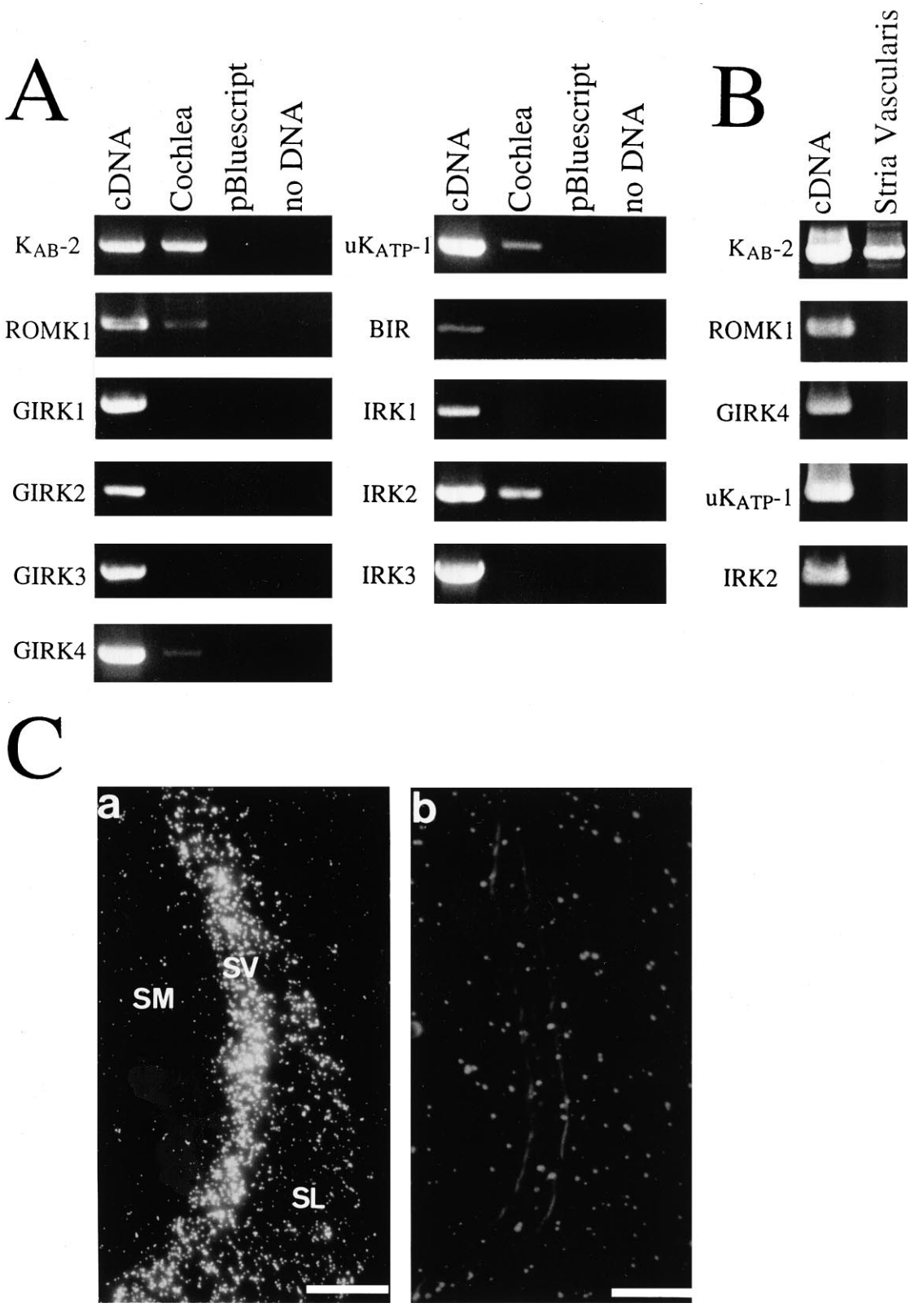

Figure 2. RT-PCR analyses and *in situ* hybridization histochemistry in rat cochlea. *A*, RT-PCR analysis of 11 Kir channel subunits in cochlea. PCR products were stained with ethidium bromide. Cochlea expressed mRNAs of K_{AB}-2, ROMK1, GIRK4, uK_{ATP}-1, and IRK2. *B*, RT-PCR analysis of Kir channel subunits in stria vascularis. PCR products were stained with SYBR Green I. Expression of only K_{AB}-2 mRNA was detected in stria vascularis. *C*, *In situ* hybridization histochemistry of K_{AB}-2 in rat cochlea. Cochlear sections were hybridized with [^{35}S]-labeled antisense cRNA (*a*) or sense cRNA (*b*). Stria vascularis expressed abundant mRNA of K_{AB}-2. *SM*, Scala media; *SV*, stria vascularis; *SL*, spiral ligament. Scale bars, 50 μm.

(Kir4.1), ROMK1 (Kir1.1), GIRK4 (Kir3.4), uK_{ATP}-1 (Kir6.1), and IRK2 (Kir2.2), were expressed in whole cochlea (Fig. 2*A*). PCR reactions with pBluescript or without DNA gave no fragment (Fig. 2*A*). We performed further RT-PCR analysis of the total RNA isolated from stria vascularis (Fig. 2*B*). Among the five subunits, only K_{AB}-2 could be detected to be expressed, even with SYBR Green I in stria vascularis (Fig. 2*B*). The nucleotide sequence of this amplified DNA fragment agreed completely with that of K_{AB}-2 (data not shown). To further ensure the absence of ROMK1, GIRK4, uK_{ATP}-1, and IRK2 in stria vascularis, we also performed RT-PCR using other sets of primers (indicated by asterisks in Table 1). We found that these primers also did not amplify their DNA fragments from RNA of stria vascularis, although in whole cochlear mRNA they detected expression of these Kir channel subunits (data not shown). We further examined the distribution of K_{AB}-2 mRNA in rat cochlea using *in situ* hybridization histochemistry (Fig. 2*C*). K_{AB}-2 mRNA was expressed strongly in stria vascularis (Fig. 2*C-a*), but little signal was detected in spiral ligament. The reaction was specific, because the sense probe of K_{AB}-2 gave no signal (Fig. 2*C-b*). Therefore, among the 11 Kir channel subunits examined so far, K_{AB}-2 is the only one expressed in stria vascularis.

Whole-mount and section immunohistochemistry

We have developed a specific polyclonal antibody against the C-terminal region of K_{AB}-2 subunit (anti-K_{AB}-2C2 antibody) (Ito et al., 1996). We examined the distribution of K_{AB}-2 in rat cochlea using this antibody (Fig. 3). Figure 3*A* shows whole-mount immunohistochemistry of rat cochlea. K_{AB}-2 immunoreactivity (*dark blue*) appeared in a "spiral"-shaped band at the lateral wall in cochlea. This spiral band of the immunoreactivity had two and one-half turns and was uniform from basal to apical portions of cochlea. These results suggest that K_{AB}-2 protein expresses homogeneously in all turns of cochlea, probably in stria vascularis (Schuknecht, 1993) (Fig. 1, *inset*). This positive reaction was not detected when preimmune serum was used (Fig. 3*B*).

Figure 3*C*,*D* demonstrates immunohistochemical localization of K_{AB}-2 in slice sections of cochlea. K_{AB}-2 immunoreactivity existed in stria vascularis in all turns of cochlea (Fig. 3*C*,*D*, *arrowheads*), as indicated in the whole-mount immunohistochemistry (Fig. 3*A*). The immunoreactivity was also detected in organ of Corti (Fig. 3*D*, *arrow*). At a higher magnification, the immunoreactivity was detected on Deiters' cells in the organ, but not in outer hair cells (data not shown). K_{AB}-2 immunoreactivity was also detected in spiral ganglions (Fig. 3*D*, *open arrow*). Careful observation revealed that this immunoreactivity was detected not in the ganglion neurons but in the satellite cells surrounding neurons (Schulte and Steel, 1994). These reactions were specific, because no immunoreactivity was detected when anti-K_{AB}-2C2 antibody with excess immunized oligopeptide was used (data not shown).

On the other hand, the vestibular dark cell area showed no immunoreactivity of K_{AB}-2 (Fig. 3*E*, *arrowheads*). Because the dark cell area in vestibule is thought to correspond to the stria vascularis in cochlea and may be responsible for the generation of high K^+-endolymph in the vestibule, this observation suggests that the K_{AB}-2 might play an important role specific to the function of stria vascularis in cochlea.

Confocal image and immunogold electron microscopy analyses of K_{AB}-2 immunoreactivity

Figure 4*A* depicts a high-power magnification of a section immunostained with anti-K_{AB}-2C2 antibody. Nuclei in this section were stained with hematoxylin. The schema of this section is shown on the left. Both intermediate (Fig. 4*A*, *asterisks*) and basal cells (Fig. 4*A*,*B, arrowheads*) were free from staining, and only marginal cells exhibited K_{AB}-2 immunoreactivity. Laser confocal microscopic examination (Fig. 4*B*) showed that K_{AB}-2 immunoreactivity (*green*) appeared as a "fold"-like structure of the basolateral side of marginal cells. The apical side facing the scala media showed no immunoreactivity (Fig. 4*B*, *arrows*). This strongly suggests that the K_{AB}-2 immunoreactivity is localized at the basolateral, but not apical, membrane of marginal cells. The fold-like appearance of immunoreactivity is consistent with the extensive invaginations of the basolateral membrane of marginal cells (Schuknecht, 1993).

The subcellular localization of K_{AB}-2 was examined further with immunoelectron microscopy of ultra-thin sections (Fig. 5). Gold particles of K_{AB}-2 immunoreactivity were detected at the invaginated basolateral membrane of marginal cells (Fig. 5*A,C*). Abundant mitochondria and invaginated membrane are features of the basolateral side of marginal cells (Schuknecht, 1993). No gold particles were detected at the apical membrane of marginal cells (Fig. 5*B*) and in intermediate cells (Fig. 5*C*, *arrows*). These results clearly indicate that K_{AB}-2 is distributed specifically at the basolateral membrane of marginal cells.

It has been suggested that cochlear marginal cells and vestibular dark cells share the same transporters and ion channels, such as Na^+,K^+-ATPase, Na^+,K^+,Cl^- cotransporter, a nonselective cation channel and a Cl^- channel (for review, see Wangemann, 1995). No difference in the ion-transport systems between cochlear marginal and vestibular dark cells has been reported. Thus the K_{AB}-2 is the first ion-transport molecule that is shown to exist in cochlear marginal cells but not in vestibular dark cells (Fig. 3*E*).

Developmental expression of K_{AB}-2 immunoreactivity

It was reported that both EP and the concentrations of K^+ ($[K^+]$) in cochlear endolymph were elevated after birth, but EP started to become positive after endolymphatic $[K^+]$ reached the adult level, as indicated in the top panel in Figure 6*A* (quoted from Anniko, 1985). We examined the developmental change of K_{AB}-2 immunoreactivity in stria vascularis at various postnatal days and compared it with elevation of $[K^+]$ and EP (Fig. 6*A,B*). At 1 and 5 d after birth, no K_{AB}-2 immunoreactivity was detected (Fig. 6*A*). At 8 d, weak immunoreactivity was detected only at the basal side of marginal cells. The immunoreactivity appeared simultaneously in stria vascularis in all turns of cochlea (Fig. 6*B*). The expression of K_{AB}-2 then increased rapidly during the following days (*P10* and *P12* in Fig. 6*A*). At 14 d, abundant staining of K_{AB}-2 protein was observed at the basolateral side, probably on the infolded basolateral membrane, similar to that of adult rats (Fig. 6*A*,*B*). The time course of K_{AB}-2 expression was closely correlated with that of the elevation of EP but not of endolymphatic $[K^+]$ (Fig. 6*A*). It is also noteworthy that developmental expression of K_{AB}-2 in satellite cells surrounding ganglion neurons seemed to be comparable with that in marginal cells (Fig. 6*B*).

W^V/W^V mutant mice expressed no K_{AB}-2 in stria vascularis

W^V/W^V mice were reported to be deaf because of the loss of the positive EP (Steel et al., 1987; Steel and Barkway, 1989). We compared K_{AB}-2 expression in cochleae between normal and W^V/W^V mice (Fig. 7).

The structure of cochlea of mouse was essentially identical to that of rat (Fig. 7*A-a*). The K_{AB}-2 immunoreactivity in mouse

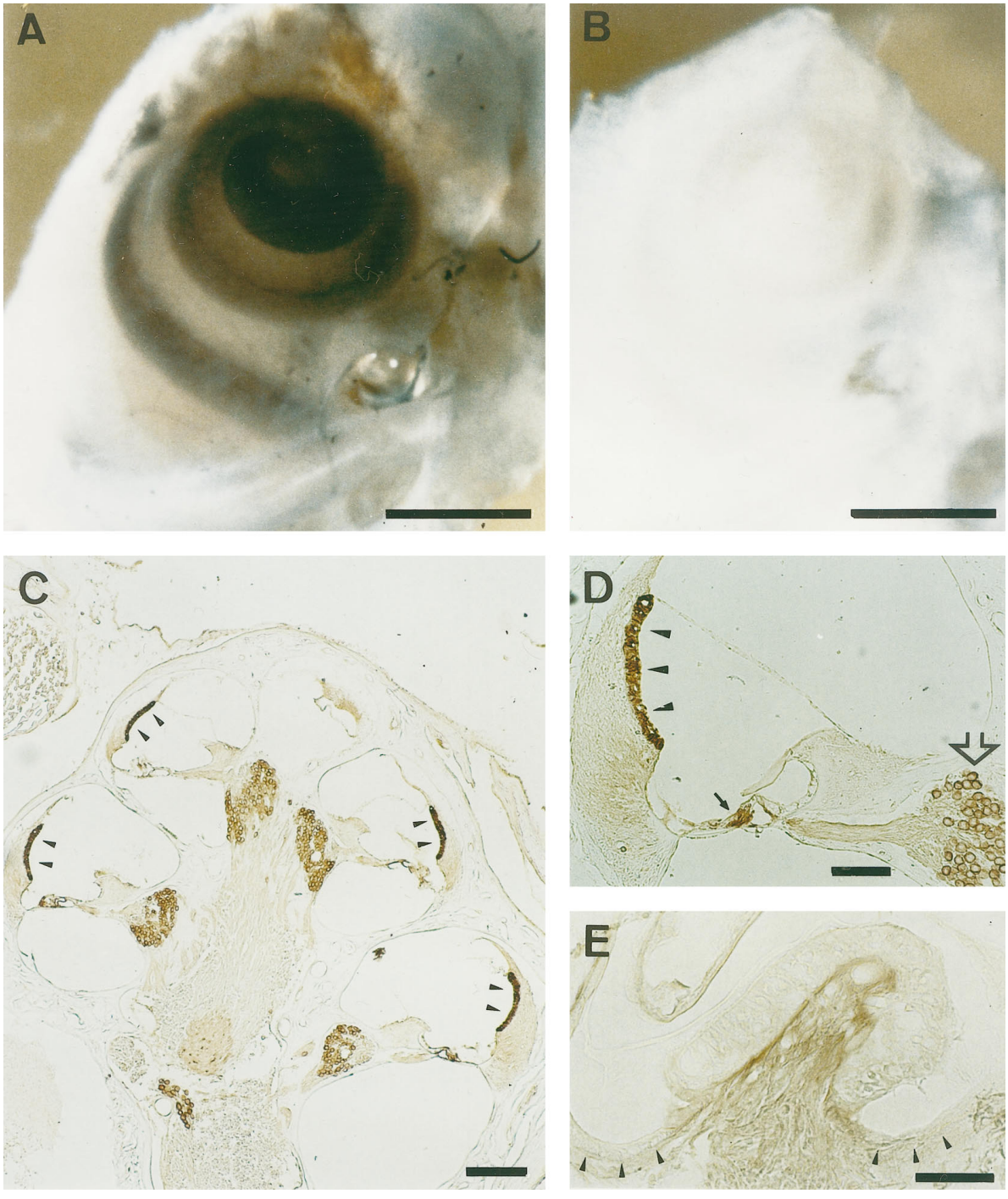

Figure 3. Immunohistochemistry of inner ear with anti-K_{AB}-2C2 antibody. *A*, *B*, Whole-mount immunohistochemistry with anti-K_{AB}-2C2 antibody (*A*) and preimmune serum (*B*). *C*, *D*, Slice immunohistochemistry. Stria vascularis of all turns was stained (*C*, *arrowheads*). At higher magnification (*D*), positive staining was detected in stria vascularis (*arrowheads*), satellite cells surrounding spiral ganglion neurons (*open arrow*), and Deiters' cells (*arrow*). *E*, Vestibular dark cell area (*arrowheads*). No K_{AB}-2 immunoreactivity was detected. Scale bars: *A*, *B*, 1 mm; *C*, 200 μm; *D*, 100 μm; *E*, 50 μm.

cochlea was detected in stria vascularis, satellite cells, and Deiters' cells as in rat (Figs. 3*D*, 7*A-a*). On the other hand, the stria vascularis of W^V/W^V mouse was poorly developed and did not exhibit prominent invaginations of basolateral membrane of marginal cells as reported previously (Fig. 7*A-b*) (Steel and Barkway, 1989). In W^V/W^V mouse, K_{AB}-2 was not detected in the stria vascularis (Fig. 7*A-b*, *arrowheads*), whereas its immunoreactivity in satellite cells remained almost the same as control (Fig. 7*A-a*, *A-b*, *open arrows*).

Next, we performed double-immunostaining of K_{AB}-2 and β2 subunit of Na^+,K^+-ATPase (Fig. 7*B*). In the control mouse, the Na^+,K^+-ATPase staining showed a prominent infolding shape at the basolateral membrane of marginal cells (Fig. 7*B-b*), as reported previously (Schulte and Steel, 1994; ten Cate et al., 1994), and seemed to be colocalized with the K_{AB}-2 immunoreactivity, as shown in the double-staining (Fig. 7*B-c*). In the stria of W^V/W^V mouse, although K_{AB}-2 immunoreactivity was completely lost (Fig. 7*B-e*), Na^+,K^+-ATPase immunoreactivity could be detected

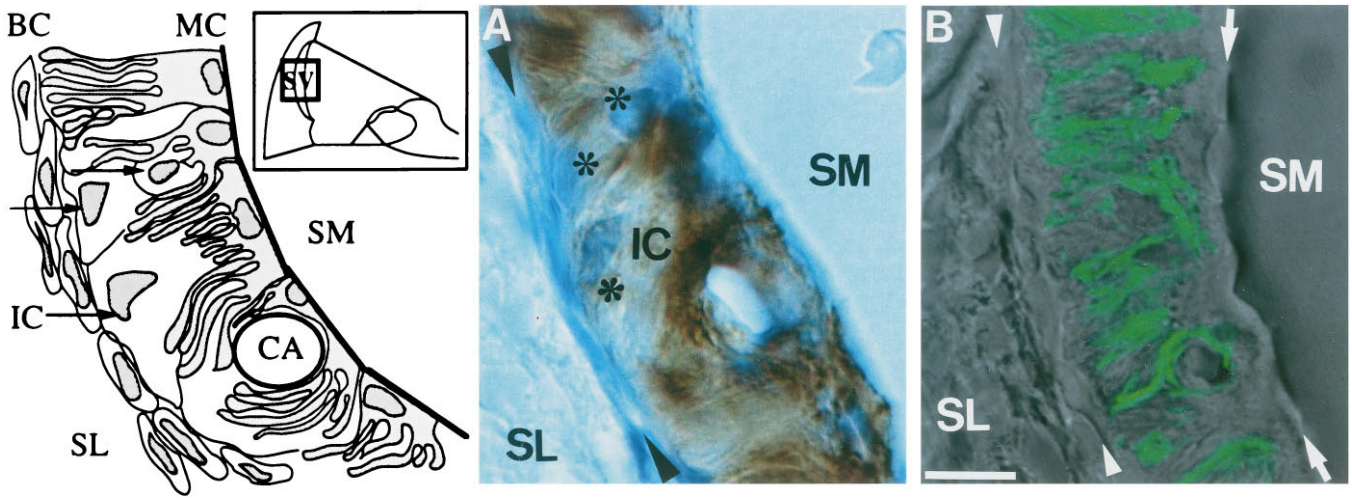

Figure 4. Immunohistochemistry of K_{AB}-2 in stria vascularis. K_{AB}-2 immunoreactivity was visualized by the DAB–ABC method (*A*) or FITC-conjugated secondary antibody (*B*). *A*, Nuclei were stained with hematoxylin. *B*, Confocal image. Positive staining was observed only at the basolateral membrane of marginal cells. Note no immunoreactivity at the apical membrane of marginal cells (*B, arrows*), in intermediate cells (*A*, *asterisks*), or in the layer of basal cells (*A, B, arrowheads*). The schema of *A* is shown on the *left*. Intermediate cells are indicated by *arrows* in the schema. *MC*, Marginal cell; *IC*, intermediate cell; *BC*, basal cell; *SV*, stria vascularis; *SL*, spiral ligament; *SM*; scala media; *CA*, capillary. Scale bar, 10 μm.

at the basolateral side of marginal cells but was weaker than that of control mouse (Fig. 7*B-f*) (Schulte and Steel, 1994).

DISCUSSION

Putative functional role of K_{AB}-2 in formation of EP

In this study, we first confirmed the results of Marcus et al. (1985) that Ba^{2+} ions injected into a vertebral artery suppressed EP. Furthermore, we found that high concentrations of blockers of K_V channels, i.e., 4-AP and TEA, had little effect on EP. Because Ba^{2+} is an effective blocker of Kir channels, it is strongly suggested that some Kir channels, but not K_V channels, are involved in the formation of positive EP. Among 11 members of Kir channel subunits, which cover almost all functional Kir channels cloned so far, we detected expression of ROMK1, GIRK4, uK_{ATP}-1, IRK2, and K_{AB}-2 mRNAs in cochlea, but only K_{AB}-2 mRNA in stria vascularis in the present conditions (see Materials and Methods). Several other reports on Kir subunits in the inner ear have appeared recently. Chick IRK1 (cIRK1, a variant of IRK1) and BIR10 (K_{AB}-2/Kir4.1) were cloned from chick cochlear hair cells (Navaratnam et al., 1995) and from cultured rat outer hair cells (Glowatzki et al., 1995), respectively. Nevertheless, K_{AB}-2 is the only Kir channel subunit identified so far to be expressed in stria vascularis. Thus, K_{AB}-2 is one candidate for the K^+ channel responsible for Ba^{2+} inhibition of EP, although a possibility still remains that Kir channel subunits that have not yet been cloned also exist in the stria vascularis.

Salt et al. (1987) discovered that the extracellular fluid in the space between the layer of marginal cells and that of basal cells (interlayer space) in stria vascularis has a potential of approximately +100 mV with its $[K^+]$ of ~5–10 mM. They proposed that the layer of basal cells is essential for maintenance of the potential difference between the interlayer space and perilymph, which may be the source of positive EP. On the other hand, the potential of vestibular endolymph, which contains 150 mM $[K^+]$, is ~0 mV, probably because the vestibular dark cell area consists of a single layer of dark cells and lacks the layer of basal cells (for review, see Wangemann, 1995). Furthermore, previous studies have indicated that cochlear marginal cells and vestibular dark cells shared identical ion-transport molecules and ion channels (Wangemann, 1995). It was speculated, therefore, that the Ba^{2+}-sensitive K^+ channel was localized at the apical membrane of basal cells. This speculation has been widely accepted (Wangemann, 1995). In this study, however, we showed that the only Kir channel subunit identified in stria vascularis, K_{AB}-2, existed in marginal cells but not in vestibular dark cells. Thus, the presumption that marginal and dark cells share identical ion-transport molecules, which has been one basis for their speculation, is no longer valid. The role of K_{AB}-2 in marginal cells should be taken into account in consideration of formation of EP.

The blockers applied through a vertebral artery probably reach the basolateral side of marginal cells, the apical side of basal cells, and intermediate cells in stria vascularis. Because we showed that K_{AB}-2 immunoreactivity in stria vascularis was specifically at the basolateral membrane of marginal cells, the Ba^{2+} ions applied through a vertebral artery could reach the K_{AB}-2 channels and inhibit them. Therefore, K_{AB}-2 channels at the basolateral membrane of marginal cells should be responsible, at least partly, for Ba^{2+}-suppression of EP, as initially proposed by Marcus et al. (1985). Other kinds of K^+ channels than Kir may exist at the basolateral membrane of marginal cells and also at the apical membrane of basal cells; however, these putative K^+ channels may not be responsible for Ba^{2+} suppression of EP, because other types of K^+ channels, such as K_V channels and Ca^{2+}-activated K^+ channels, are relatively insensitive to Ba^{2+} and/or can be inhibited by high concentrations of 4-AP or TEA (Osterrieder et al., 1982; Benham et al., 1985; for review, see Pongs, 1992). A possibility still remains, however, that unknown Kir channel subunits may exist in stria vascularis and may be involved in Ba^{2+}-suppression of EP. To obtain the final conclusion that K^+ channels are involved in Ba^{2+} suppression of EP, it is necessary to fully characterize the functional K^+ channels at the basolateral membrane of marginal cells and also at the apical membrane of basal cells, using patch-clamp technique.

Because both the potential of marginal cells and that of extracellular fluid in the interlayer space is approximately +100

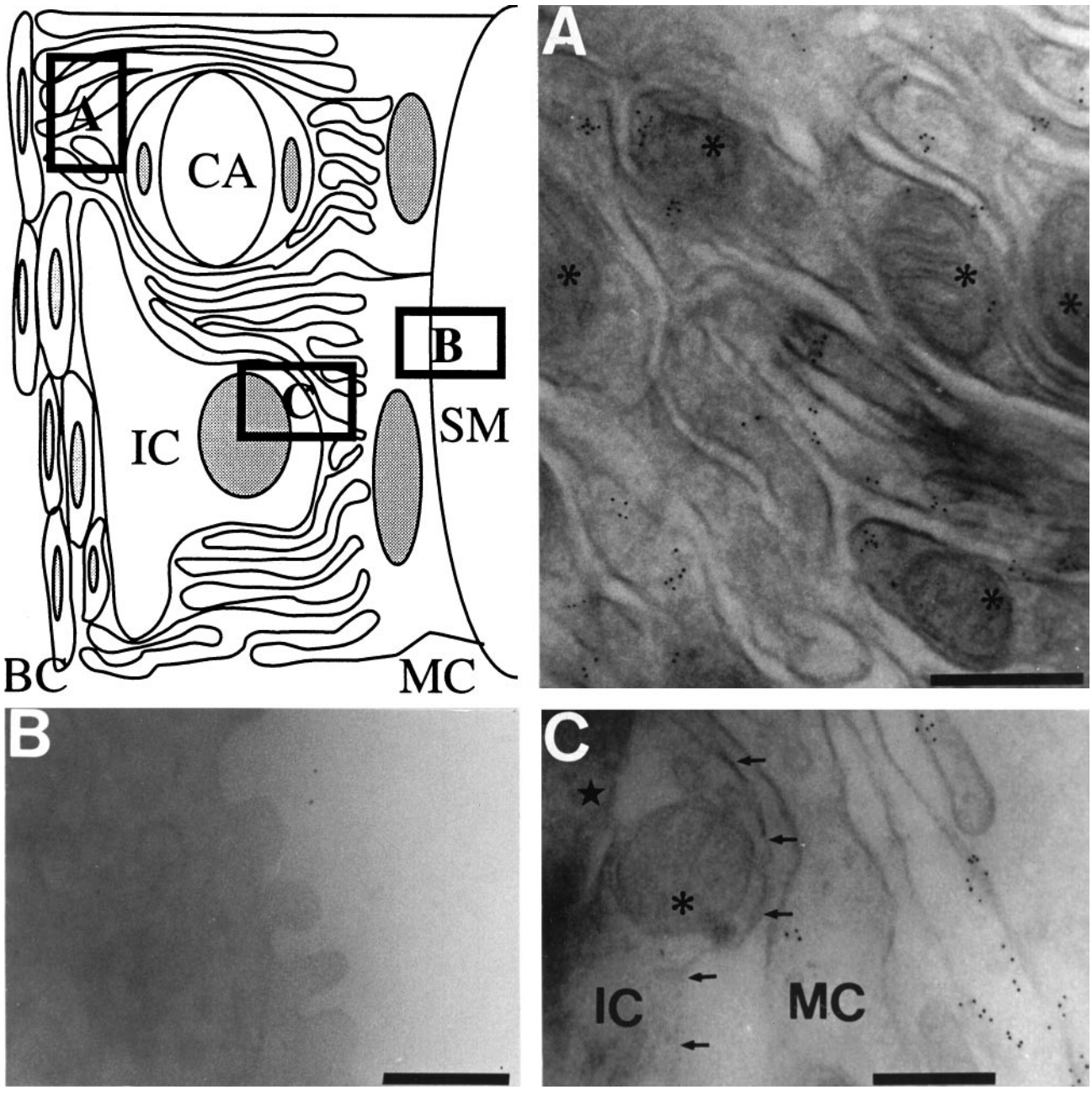

Figure 5. Immunogold electron microscopic examination of K_{AB}-2 in stria vascularis. *A–C*, Electron microscopic images of the portions as indicated in the *top left* schema. Positive gold particles were observed only at the basolateral membrane of marginal cells (*A*, *C*), but at neither the apical membrane of marginal cells (*B*) nor the membrane of intermediate cells (*C*, *arrows*). *Asterisks* show mitochondria, which exist abundantly in the basolateral foldings of marginal cells (*A*). *SM*, Scala media; *MC*, marginal cell; *IC*, intermediate cell; *BC*, basal cell; *CA*, capillary; *asterisks*, mitochondria; *star*, nucleus. Scale bars: *A–C*, 0.25 μm.

mV, and because this extracellular fluid contains ~5–10 mM $[K^+]$ (Salt et al., 1987), K^+ ions should flow through K_{AB}-2, at least theoretically, outward from the basolateral side of marginal cells to the extracellular space. Abundant Na^+,K^+-ATPase and $Na^+,K^+,2Cl^-$ cotransporter are localized at the basolateral membrane of marginal cells. These ion-transport molecules, when working actively, may cause depletion of K^+ ions in the extracellular fluid surrounded by the prominent infoldings of basolateral membrane of marginal cells (Fig. 5), which may result in inhibition of these ion transporters. To sustain high activity of Na^+,K^+-ATPase and $Na^+,K^+,2Cl^-$ cotransporter, K^+ secretion through K_{AB}-2 into interlayer space from marginal cells may be mandatory. This function of K_{AB}-2 in stria vascularis is comparable with that in renal distal tubules, where K_{AB}-2 is colocalized with Na^+,K^+-ATPase at the basolateral membrane of renal epithelial cells (Ito et al., 1996). K_{AB}-2 in renal epithelial cells probably secretes K^+ ions into the narrow spaces surrounded by the infoldings of epithelial basolateral membrane to sustain the activity of Na^+,K^+-ATPase (for review, see Giebisch, 1995). Ba^{2+} inhibition of EP thus might be explained as follows. Ba^{2+} ions, applied into a vertebral artery, may inhibit K_{AB}-2 channels at the basolateral

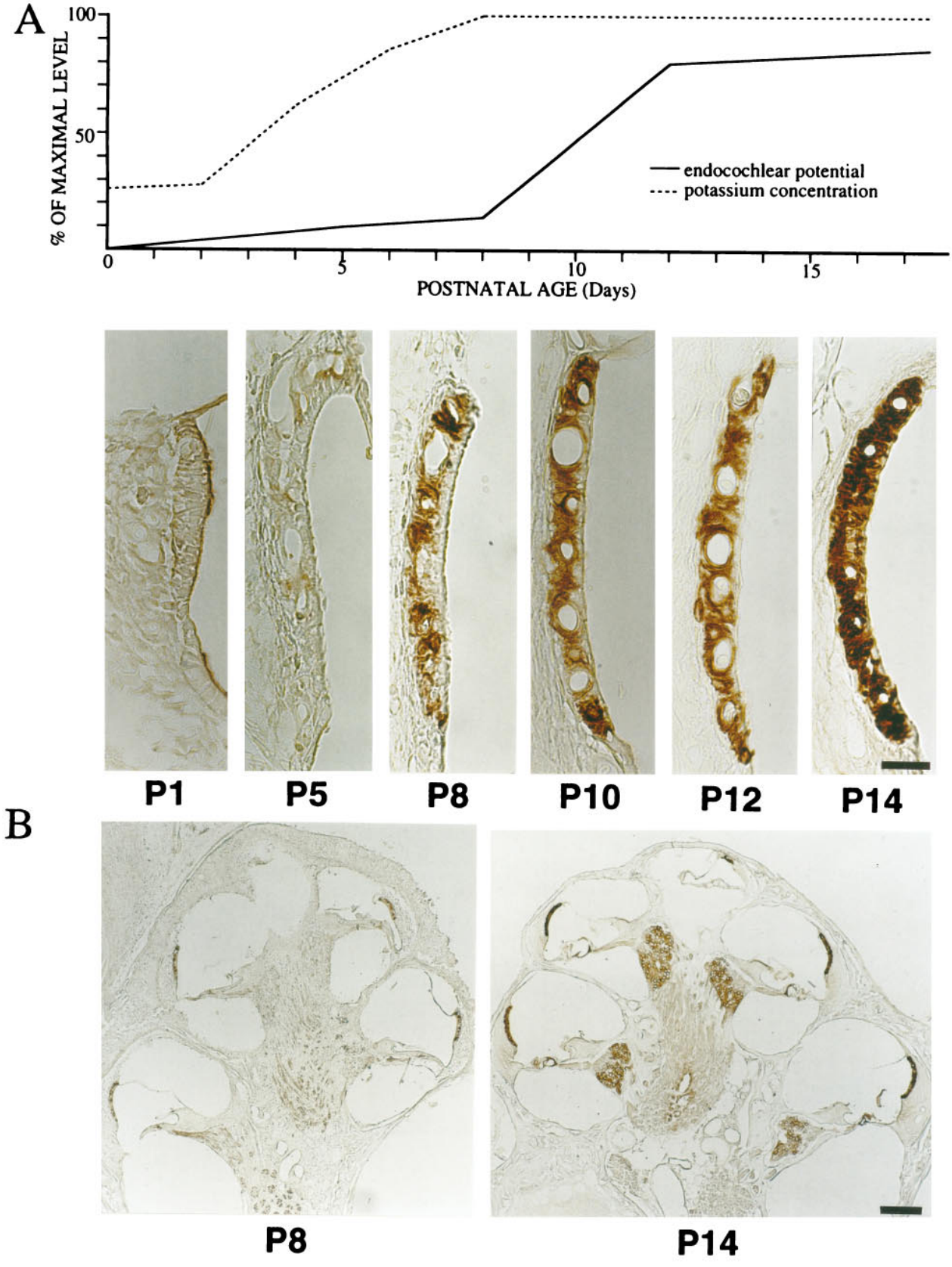

Figure 6. Developmental studies of the expression of K_{AB}-2 in marginal cells. *A*, Comparison of developmental change of K_{AB}-2 expression in stria vascularis with elevation of EP and that of endolymphatic $[K^+]$ in postnatal rats. The lines of EP and $[K^+]$ shown in the *top panel* were obtained from a review (Anniko, 1985). *B*, Sagittal sections of cochlea at various postnatal days. Note that expression of K_{AB}-2 in satellite cells is comparable with that in stria vascularis. All sections of *A* and *B* were stained with the ABC–DAB method. Scale bars: *A*, 25 μm; *B*, 200 μm.

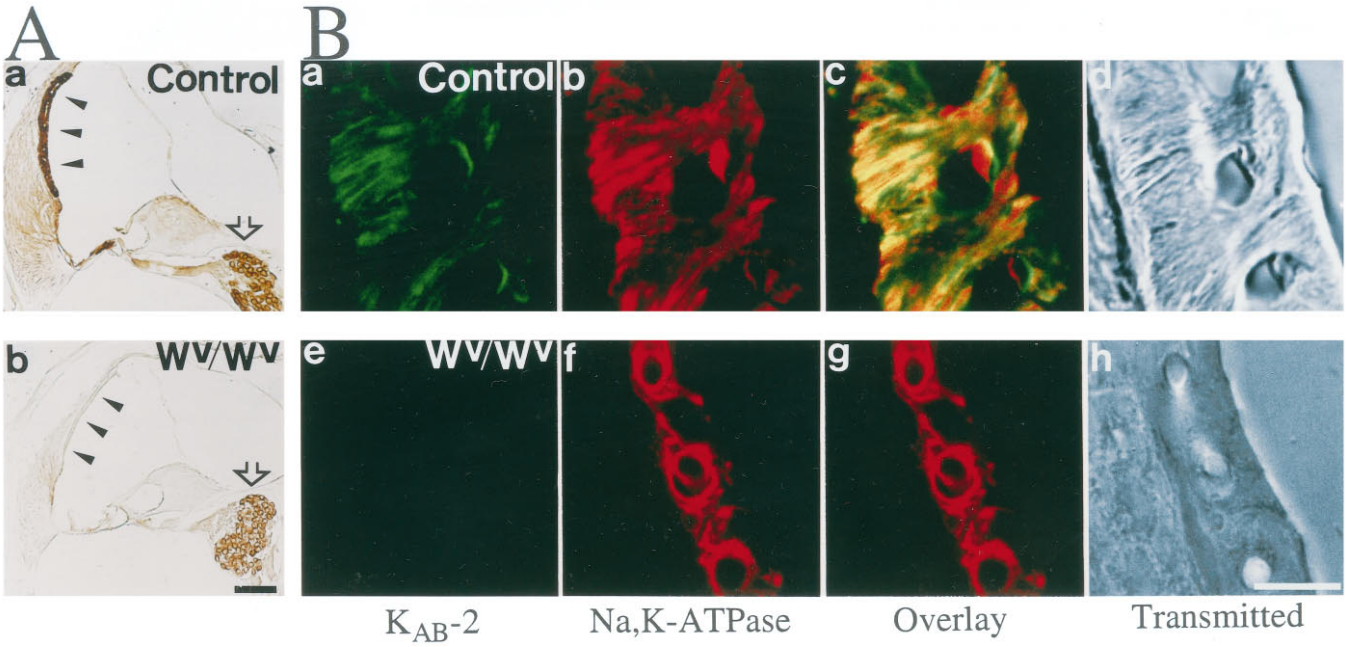

Figure 7. Expression of K_{AB}-2 in normal mice and W^V/W^V mutant mice. *A*, Immunostaining of K_{AB}-2 in normal mouse (*a*) and W^V/W^V mouse (*b*) with the DAB–ABC method. Note that in W^V/W^V mouse, K_{AB}-2 immunoreactivity was not observed in stria vascularis (*b*, *arrowheads*), but it was detected in satellite cells (*b*, *open arrow*) as much as control (*a*, *open arrow*). *B*, Double-immunostaining of K_{AB}-2 and β2 subunit of Na^+,K^+-ATPase in stria vascularis. The *top* (*a–d*) and *bottom panels* (*e–h*) show the immunohistochemistry of control mouse and that of W^V/W^V mouse, respectively. In control mouse, both the immunoreactivity of K_{AB}-2 (*a*) and that of Na^+,K^+-ATPase (*b*) were detected and seemed to be colocalized at the basolateral membrane of marginal cells (*c*). On the other hand, in W^V/W^V mouse, the immunoreactivity of K_{AB}-2 was not detected (*e*), although that of Na^+,K^+-ATPase was expressed moderately (*f, g*). *d* and *h* are transmitted images of stria vascularis. These were consistent findings in all eight mutant mice examined. Scale bars: *A*, 100 μm; *B*, 10 μm.

membrane of marginal cells, which diminishes the supply of K^+ ions to Na^+,K^+-ATPase and $Na^+,K^+,2Cl^-$ cotransporter, inhibits them, and finally suppresses EP.

Expression of K_{AB}-2 during development and in deaf mutant mice

The relationship between elevation of EP and expression of K_{AB}-2 in normal development after birth also supports the idea that K_{AB}-2 may be important for the generation of EP. For several days after birth when K_{AB}-2 was not expressed, EP was reported to be very low, although Na^+,K^+-ATPase should have already been expressed moderately, and endolymphatic $[K^+]$ started to elevate (Anniko, 1985; Yao et al., 1994). It was also reported that the adult level of endolymphatic $[K^+]$ and that of Na^+,K^+-ATPase had been established before EP reached its maximum plateau, whereas the developmental expression of K_{AB}-2 shown in this study paralleled the reported time course of elevation of EP (Yao et al., 1994) (Fig. 6). These results strongly suggest the importance of K_{AB}-2 in the formation of EP. It seems probable that moderate expression of Na^+,K^+-ATPase is sufficient to elevate endolymphatic $[K^+]$ but insufficient to elevate EP. High-level expression of Na^+,K^+-ATPase may be needed for elevation of EP, which may essentially require K_{AB}-2 for supply of K^+ ions to the K^+ site of the ATPase. Thus, the expression of K_{AB}-2 in marginal cells might be induced by the demand of high activity of Na^+,K^+-ATPase. The regulatory mechanism of expression of K_{AB}-2 is unknown, however, and further studies are definitely needed.

We found that in W^V/W^V, K_{AB}-2 was not expressed in stria vascularis but exhibited normal expression in spiral ganglions. Therefore, the loss of K_{AB}-2 in the marginal cells of W^V/W^V may not be caused by abnormalities of the K_{AB}-2 gene itself, but may be secondary to abnormality in differentiation of marginal cells. Consistent with this notion, we found that the stria vascularis in W^V/W^V was thin, and its marginal cells did not develop much infolding of their basolateral membrane as in the early stages of development of control mice (Steel and Barkway, 1989). The expression of Na^+,K^+-ATPase in these marginal cells was also moderate (Schulte and Steel, 1994) (Fig. 7). Thus, similar to the early stages of normal development, the moderate expression of Na^+,K^+-ATPase alone in W^V/W^V may be insufficient for elevation of EP. The mechanism responsible for poor differentiation of the stria vascularis in W^V/W^V is unknown but might be related to the absence of intermediate cells in this mutant (Steel et al., 1987); it is known that melanocytes, to which intermediate cells belong, play essential roles in normal differentiation of various tissues (Mayer, 1970). Further studies are needed to clarify the mechanism of normal differentiation of marginal cells and its relation to expression of K_{AB}-2.

Localization mechanism of K_{AB}-2 at basolateral membrane of epithelia

K_{AB}-2 immunoreactivity was detected specifically at the basolateral membrane of cochlear marginal cells and distal convoluted renal epithelial cells (Ito et al., 1996). Recently, several mechanisms that determine subcellular localization of membrane proteins have been identified (Rothmann and Wieland, 1996). Low-density lipoprotein receptor has tyrosine-containing motifs in its C terminus that are necessary to sort the receptor to basolateral membrane (Matter et al., 1993). It is considered that Na^+,K^+-ATPase is localized at the basolateral membrane of epithelial cells by binding to the fodorin–ankyrin system via a motif of Ala–Leu–

Leu–Lys (Jordan et al., 1995). PSD-95/SAP90 and its homologs have been shown to cluster various receptors and ion channels whose C termini possess a motif of Thr/Ser–X–Val (Kim et al., 1995; Kornau et al., 1995; Gomperts, 1996). K_{AB}-2 has the motif of Ser–Asn–Val in its C-terminal end but not that of Ala–Leu–Leu–Lys. Because SAP97, one of the PSD-95/SAP90 family, was expressed at the basolateral membrane of epithelial cells of small intestine and choroid plexus (Müller et al., 1995), it is possible that PSD-95/SAP90 family proteins in marginal cells are responsible for the localization of K_{AB}-2 at their basolateral membrane. Further studies are needed, however, to elucidate the molecular mechanism responsible for subcellular localization of K_{AB}-2 at the basolateral membrane of marginal cells.

REFERENCES

Anniko M (1985) Histochemical, microchemical (microprobe) and organ culture approaches to the study of auditory development. Acta Otolaryngol (Stockh) [Suppl] 421:10–18.

Ashmore JF (1991) The electrophysiology of hair cells. Annu Rev Physiol 53:465–476.

Benham CD, Bolton TB, Lang RJ, Takewaki T (1985) The mechanism of action of Ba^{2+} and TEA on single Ca^{2+}-activated K^+-channels in arterial and intestinal smooth muscle cell membranes. Pflüger Arch 403:120–127.

Bond CT, Pessia M, Xia X-M, Lagrutta A, Kavanaugh MP, Adelman JP (1994) Cloning and expression of a family of inward rectifier potassium channels. Receptors Channels 2:183–191.

Dallos P (1978) Cochlear electrophysiology. In: Evoked electrical activity in the auditory nervous system (Naunton RF, Fernandez C, eds), pp 141–150. San Diego: Academic.

Doupnik CA, Davidson N, Lester HA (1995) The inward rectifier potassium channel family. Curr Opin Neurobiol 5:268–277.

Giebisch G (1995) Renal potassium channels: an overview. Kidney Int 48:1004–1009.

Glisin V, Crkvenjakov R, Byus C (1974) Ribonucleic acid isolated by cesium chloride centrifugation. Biochemistry 13:2633–2637.

Glowatzki E, Fakler G, Brändle U, Rexhausen U, Zenner H-P, Ruppersberg JP, Fakler B (1995) Subunit-dependent assembly of inward-rectifier K^+ channels. Proc R Soc Lond [Biol] 261:251–261.

Gomperts SN (1996) Clustering membrane proteins: it's all coming together with the PSD-95/SAP90 protein family. Cell 84:659–662.

Gotow T, Tanaka J, Takeda M (1995) The organization of neurofilaments accumulated in perikaryon following aluminum administration: relationship between structure and phosphorylation of neurofilaments. Neuroscience 64:553–569.

Ito M, Inanobe A, Horio Y, Hibino H, Isomoto S, Ito H, Mori K, Tonosaki A, Tomoike H, Kurachi Y (1996) Immunolocalization of an inwardly rectifying K^+ channel, K_{AB}-2 (Kir4.1), in the basolateral membrane of distal renal tubular epithelia. FEBS Lett 388:11–15.

Jordan C, Püschel B, Koob R, Drenckhahn D (1995) Identification of a binding motif for ankyrin on the α-subunit of Na^+,K^+-ATPase. J Biol Chem 270:29971–29975.

Kim E, Niethammer M, Rothschild A, Jan YN, Sheng M (1995) Clustering of Shaker-type K^+ channels by interaction with a family of membrane-associated guanylate kinases. Nature 378:85–88.

Konishi T, Mendelsohn M (1970) Effect of ouabain on cochlear potentials and endolymph composition in guinea pigs. Acta Otolaryngol (Stockh) 69:192–199.

Kornau H-C, Schenker LT, Kennedy MB, Seeburg PH (1995) Domain interaction between NMDA receptor subunits and the postsynaptic density protein PSD-95. Science 269:1737–1740.

Kusakari J, Comegys TH, Thalmann I, Thalmann R (1978) Effect of ethacrynic acid, furosemide, and ouabain upon the endolymphatic potential and upon high energy phosphates of the stria vascularis. Laryngoscope 88:12–37.

Marcus DC, Rokugo M, Thalmann R (1985) Effects of barium and ion substitutions in artificial blood on endocochlear potential. Hear Res 17:79–86.

Marcus DC, Liu J, Wangemann P (1994) Transepithelial voltage and resistance of vestibular dark cell epithelium from the gerbil ampulla. Hear Res 73:101–108.

Matter K, Whitney JA, Yamamoto EM, Mellman I (1993) Common signals control low density lipoprotein receptor sorting in endosomes and the golgi complex of MDCK cells. Cell 74:1053–1064.

Mayer TC (1970) A comparison of pigment cell development in albino, steel, and dominant-spotting mutant mouse embryos. Dev Biol 23:297–309.

Morgenstern C, Amano H, Orsulakova A (1982) Ion transport in the endolymphatic space. Am J Otolaryngol 3:323–327.

Müller BM, Kistner U, Veh RW, Cases-Langhoff C, Becker B, Gundelfinger ED, Garner CC (1995) Molecular characterization and spatial distribution of SAP97, a novel presynaptic protein homologous to SAP90 and the *Drosophila* discs-large tumor suppressor protein. J Neurosci 15:2354–2366.

Navaratnam DS, Escobar L, Covarrubias M, Oberholtzer JC (1995) Permeation properties and differential expression across the auditory receptor epithelium of an inward rectifier K^+ channel cloned from the chick inner ear. J Biol Chem 270:19238–19245.

Osterrieder W, Yang Q-F, Trautwein W (1982) Effects of barium on the membrane currents in the rabbit S-A node. Pflügers Arch 394:78–84.

Pongs O (1992) Molecular biology of voltage-dependent potassium channels. Physiol Rev [Suppl] 72:S69–S88.

Rothman JE, Wieland FT (1996) Protein sorting by transport vesicles. Science 272:227–234.

Salt AN, Melichar I, Thalmann R (1987) Mechanisms of endocochlear potential generation by stria vascularis. Laryngoscope 97:984–991.

Schuknecht HF (1993) Anatomy. In: Pathology of the ear (Schuknecht HF, ed), pp 31–75. Malvern, PA: Lea & Febiger.

Schulte BA, Adams JC (1989) Distribution of immunoreactive Na^+,K^+-ATPase in gerbil cochlea. J Histochem Cytochem 37:127–134.

Schulte BA, Steel KP (1994) Expression of α and β subunit isoforms of Na,K-ATPase in the mouse inner ear and changes with mutations at the W^V or Sl^d loci. Hear Res 78:65–76.

Steel KP, Barkway C (1989) Another role for melanocytes: their importance for normal stria vascularis development in the mammalian inner ear. Development 107:453–463.

Steel KP, Barkway C, Bock GR (1987) Strial dysfunction in mice with cochleo-saccular abnormalities. Hear Res 27:11–26.

Takumi T, Ishii T, Horio Y, Morishige K-I, Takahashi N, Yamada M, Yamashita T, Kiyama H, Sohmiya K, Nakanishi S, Kurachi Y (1995) A novel ATP-dependent inward rectifier potassium channel expressed predominantly in glial cells. J Biol Chem 270:16339–16349.

Tasaki I, Spyropoulos CS (1959) Stria vascularis as source of endocochlear potential. J Neurophysiol 22:149–155.

ten Cate W-JF, Curtis LM, Rarey KE (1994) Na,K-ATPase α and β subunit isoform distribution in the rat cochlear and vestibular tissues. Hear Res 75:151–160.

Wangemann P (1995) Comparison of ion transport mechanisms between vestibular dark cells and strial marginal cells. Hear Res 90:149–157.

Yao X, ten Cate W-JF, Curtis LM, Rarey KE (1994) Expression of Na^+,K^+-ATPase α1 subunit mRNA in the developing rat cochlea. Hear Res 80:31–37.

Yoshida H, Kunisada T, Kusakabe M, Nishikawa S, Nishikawa S-I (1996) Distinct stages of melanocyte differentiation revealed by analysis of nonuniform pigmentation patterns. Development 122:1207–1214.